PERGAMON

Solid State Communications 115 (2000) 149–154

solid state communications

www.elsevier.com/locate/ssc

The photoelectric conversion of the dichromophore quinolinium dye from the monolayer modified ITO electrode

Deng-Guo Wu, Chun-Hui Huang*, Jie Zheng, Yan-Yi Huang

State Key Laboratory of Rare Earth Materials Chemistry and Applications, PKU-HKU Joint Laboratory on Rare Earth Material and Bioinorganic Chemistry, Peking University, Beijing 100871, People's Republic of China

Received 15 October 1999; accepted 15 March 2000 by Z.Z. Gan

Abstract

Two dichromophore dye molecules, 4,4′-di-{1-[1-(*N*,*N*-dioctadecaneamino)phenylethylquinolinium bromine]-propyl}-dipyridinium bromine (QMV_3) and 4,4′-di-{1-[1-(*N*,*N*-dioctadecaneamino)phenylethylquinolinium bromine]-octyl}-dipyridinium bromine (QMV_8) were synthesized and transferred onto an ITO electrode using the Langmuir–Blodgett (LB) technique. The photocurrent generation was investigated versus applied electrode potential, concentration of the electron acceptors or donor, and pH of the electrolyte. A mechanism of light-induced electron injection is proposed. © 2000 Published by Elsevier Science Ltd. All rights reserved.

Keywords: A. Thin films; A. Semiconductors; D. Photoconductivity and photovoltaics

1. Introduction

Spectral sensitization of semiconductors has been a wide and very active field of research during the last three decades, driven mainly by its importance in photographic processes and solar energy conversion [1]. Much attention has been paid to mechanisms of sensitization [2,3] and the design of new systems [4]. It is known that methyl viologen diiodide (MV^{2+}) acted as a better electron acceptor in the photoelectrochemical system and it plays an important role in the charge separation and electron transfer [5]. And our group recently found that the non-linear optic material quinolinium dyes [6,7] also have photoelectric conversion property [8]. To understand further the relationship between the structure and photocurrent generation, as part of our systematic studies, we designed the two quinolinium dye dichromophores, which are also connected with the viologen derivative through different lengths of methene chains. For comparison, 1-methyl-4-[(*N*,*N*-dioctadecaneamino)phenylethyle]quinolinium iodide (QMV) was also synthesized (Scheme 1). In this paper, their photoelectric response was investigated. A mechanism rationalizing all the observations is suggested.

2. Experimental section

2.1. Materials

4,4′-Dipyridyl,1,3-dibromopropane, and 1,8-dibromooctane are from Fluka, all the commercially available reagents are A.R grade and were used as received unless indicated. Water ($R \sim 18\ M\Omega$) from an EASYpure RF system was used to prepare the LB films.

2.2. Synthesis

4-(Dioctadecaneamino) benzaldehyde was synthesized according to the previous method reported [9]. The viologen derivatives were synthesized by the reaction of 4,4′-dipyridyl with 1,3-dibromopropane or 1,8-dibromooctane in absolute ethanol. 4,4′-Di-[1-(4-methyle-quinolinium bromine)-propyl]-dipyridinium bromine was synthesized by the reaction of 4,4′-di-(1-bromine-propyl)-dipyridinium bromine with lepidine in absolute ethanol. 4,4′-Di-{1-[1-(*N*,*N*-dioctadecaneamino)phenylethylquinolinium bromine]-propyl}-dipyridinium bromine (QMV_3) was synthesized by condensing 4,4′-di-[1-(4-methyl-quinolinium

* Corresponding author. Tel.: +86-10-6275-7156; fax: +86-10-6275-1708.

E-mail address: hch@chemms.chem.pku.edu.cn (C.-H. Huang).

0038-1098/00/$ - see front matter
PII: S0038-1098(00)00155-1

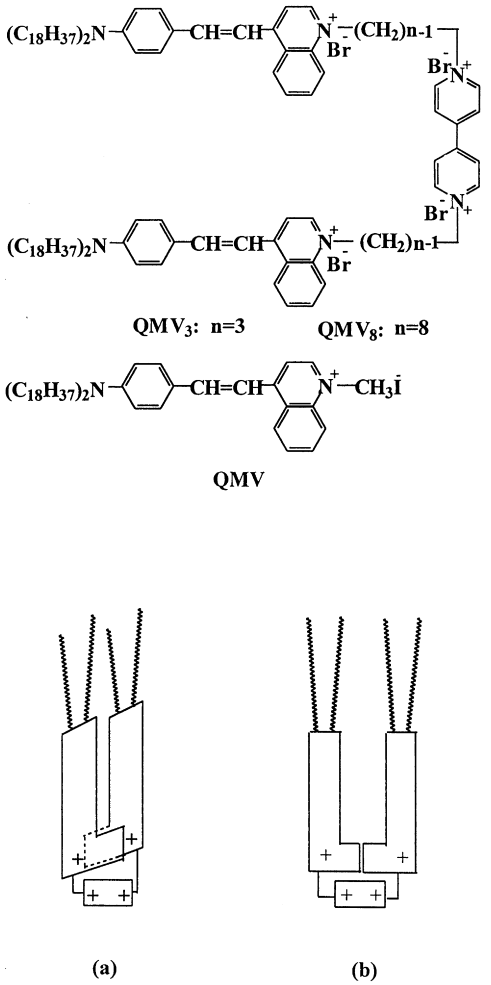

Scheme 1.

bromine)-propyl]-dipyridinium bromine with an excess of 4-(dioctadecaneamino)benzaldehyde in the mixture solvents of absolute ethanol and chloroform, using piperidine as the catalyst. 4,4′-Di-{1-[1-(*N*,*N*-dioctadecaneamino)phenylethylquinolinium bromine]-octyl}-dipyridinium bromine (QMV_8) was synthesized following the same procedure as QMV_3. QMV was synthesized by condensing *N*,*N*-dioctadecaneaminobenzaldehyde with 1,4-dimethyl-quinolinim iodide. During the entire synthesizing process, the semifinished products were purified by recrystallization, final products were purified by column chromatography under ambient conditions (eluent: chloroform–methanol, 10:1). The elemental analysis: Found for QMV_3: C, 71.16; H, 10.08; N, 4.13%. Calcd for $C_{122}H_{192}N_6Br_4$: C, 71.05; H, 9.38; N, 4.07%. ^{1}H NMR ($CDCl_3$) $\delta = 0.87$ (t, 12H, $4CH_3$), 1.20 (m, 120H, $60CH_2$), 1.70 (m, 8H, $4CH_2$), 3.18 (t, 4H, $2CH_2$), 3.19 (t, 8H, $4N–CH_2$), 5.31 (t, 8H, $4N^+–CH_2$), 6.67 (d, 4H, 2phenyl), 7.55 (d, 2H, 2-CH=), 7.96 (d, 4H, 2phenyl), 8.10 (d, 2H, 2-CH=), 8.27 (m, 4H, quinolyl), 8.48 (m, 4H, quinolyl), 8.64 (d, 2H, quinolyl), 10.0 (d, 2H, quinolyl). The elemental analysis: Found for QMV_8: C, 71.67; H, 10.12; N, 3.58%. Calcd for $C_{132}H_{212}N_6Br_4$: C, 71.97; H, 9.70; N, 3.82%. ^{1}H NMR ($CDCl_3$) $\delta = 0.87$ (t, 12H, $4CH_3$), 1.21 (m, 120H, $60CH_2$), 1.69 (m, 8H, $4CH_2$), 1.93 (t, 16H, $8CH_2$), 3.17 (t, 8H, $4N–CH_2$), 3.43 (t, 8H, $4CH_2$), 5.04 (t, 8H, $4N^+–CH_2$), 6.67 (d,4H, phenyl), 7.53 (d, 2H,2CH=), 7.65 (d, 4H, phenyl), 7.67 (d,2H, 2CH=),7.87 (m,4H,quinolyl), 8.10 (m,4H, quinolyl), 8.49 (d, 2H,quinolyl), 9.9 (d, 2H, quinolyl). The elemental analysis: Found for QMV: C, 71.50; H, 9.99; N, 3,57%. Calcd for $C_{54}H_{91}N_2I$: C, 72.45; H, 10.25; N, 3.13%, ^{1}H NMR ($CDCl_3$) $\delta = 0.87$ (t, 6H, $2CH_3$), 1.24 (m, 60H, $30CH_2$), 1.62 (m, 4H, $2CH_2$), 3.36 (t,4H, $2N–CH_2$), 4.58(s, 3H, $N^+–CH_3$), 6.68 (d, 2H, phenyl), 7.54 (d, 1H, 1CH=), 7.62 (d, 2H, phenyl), 7.75 (d, 1H, 1CH=), 7.86 (m, 2H, quinolyl), 8.0 (m,2H,quinolyl), 8.56 (d, 1H, quinolyl), 9.75 (d, 1H, quinolyl). MV^{2+} was synthesized by the reaction of 4,4′-dipyridyl with methyl iodide. Its identity was confirmed by the ^{1}H NMR analysis.

2.3. Experimental measurements

Elemental analysis and ^{1}H NMR spectrum were performed by using a Carlo Erba 1106 elemental analyzer and Brucker ARX400, respectively. Absorption spectra were measured with a Shimadzu model 3100 UV-Vis spectrophotometer. The monolayers of the dyes QMV, QMV_3 and QMV_8 were prepared by spreading it on a NIMA 622 Langmuir–Blodgett trough, and the temperature was kept constant at 20 ± 2°C. Details of the method used for pressure (π)–area (A) measurement and transfer process were the same as described previously [9]. In all cases, the ratio transfer was close to 1.0 ± 0.1.

Photoelectrochemical measurements were carried out in 0.5 M KCl solution using the LB film modified ITO electrode, platinum wire and saturated calomel electrode (SCE) as working electrode, counter electrode and reference electrode, respectively. Photocurrent was recorded with a model CH 600 voltammetry analyzer controlled by a computer. Illumination was performed with a 500 W Xe arc lamp as the light source. In order to get a given bandpass of light, the light beam was passed through a group of filters (ca. 300–800 nm, Toshiba Co, Japan, and Schott Co USA). The light intensity at each wavelength was calibrated with an energy and power meter (Scientech, USA). The effective illuminated area of a flat window was 0.38 cm^2. Cyclic voltammetry (CV) experiments was performed on an EG&GPAR 273 potentiostat/galvanostat with EG&GPAR 270 electrochemical software.

3. Results and discussion

3.1. The behavior of the dyes on water–air interface and the UV-spectra of the dyes

The pressure–area isotherms of the dyes QMV, QMV_3

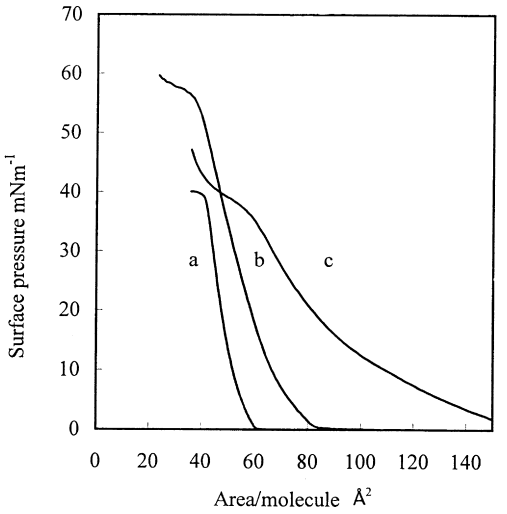

Fig. 1. Surface pressure–area (π–A) isotherms of (a) QMV, (b) QMV_3 and (c) QMV_8 at the air–water interface (20 ± 1°C).

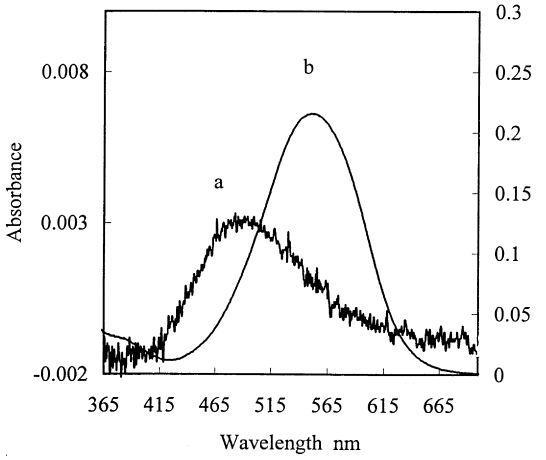

Fig. 2. UV-Vis absorption spectra of QMV_3: (a) monolayer film on ITO electrode; (b) in chloroform solution.

and QMV_8 are given in Fig. 1. As is shown, the collapse pressure of the QMV and QMV_8 are similar, ca. 40 mN m^{-1}, but that of QMV_3 is ca. 57 mN m^{-1}, which is the highest in the three dye molecules, indicating that the stability of the QMV_3 monolayer film on the water surface is the best among the three dyes. The limiting areas of QMV, QMV_3 and QMV_8 are 0.54, 0.70 and 1.06 nm^2, respectively, using a tangent to the curve at 30 mN m^{-1}. The limiting area of QMV_8 is twice that of QMV, while the limiting area of QMV_3 only increases 0.16 nm^2 in comparison with that of QMV, which may result from the different molecular alignment on the water–air interface due to the different methene chain between the chromophores and 4,4′-dipyridine (shown in Scheme 1). When QMV_3 and QMV_8 molecules were compressed on the water surface, the eight methene chains of QMV_8 can fold easily and make molecules freely align as QMV does. As a result, the limiting area of QMV_8 is as large as that of two QMV molecules, as shown in Scheme 1(b). The short methene chain leads to a larger tensile stress between the chromophores and 4,4′-dipyridine in QMV_3, than in QMV_8, and the two chromophores have to twist at an angle to form an overlapped alignment (as shown in Scheme 1(a)) during compression, thus the molecular limiting area is smaller and the stability of the monolayer is higher than in QMV_8.

Table 1 gives the maximum absorption wavelengths of the dyes in the chloroform solution and on the films, which indicates that the charge transfer bands for all the dyes are blue shifted ca. 52–64 nm when they are transferred from the solution to ITO electrodes. The blue shifts suggest the presence of H-aggregates in the films [10]. Absorption spectra of the monolayer film and the chloroform solution for QMV_3, as an example, are shown in Fig. 2.

3.2. Photocurrent responses of the dye-fabricated electrodes

Steady cathodic photocurrents were obtained, when the dye monolayer-modified ITO electrodes were illuminated with the 110 mW cm^{-2} white light. The photocurrent action spectra for QMV_3 (shown in Fig. 3), as an example, were

Table 1
Experimental data of QMV, QMV_3 and QMV_8 (I: photocurrent; φ: quantum yield; A: area/molecule; λ_{max}: maximum wavelength (l and s stand for solution and film, respectively)

Dyes	I^a (nA cm^{-2})	I^b (nA cm^{-2})	φ^b (%)	I^c (nA cm^{-2})	φ^c (%)	I^d (nA cm^{-2})	φ^d (%)	A (nm^2)	$\lambda_{max(l)}$ (nm)	$\lambda_{max(s)}$ (nm)
QMV	789.4–892.9	95.8	0.66	100.0	0.68	104.8	0.72	0.54	584	532
QMV_3	1125.4–1326.5	119.5	0.71	122.8	0.73	199.4	1.19	0.70	551	488
QMV_8	704.3–974.3	82.2	0.72	93.6	0.83	101.5	0.90	1.06	583	519

[a] Irradiation under 110 mW cm^{-2} white length, in 0.5 M KCl electrolyte solution containing 1 mM MV^{2+}.
[b] Irradiation under 464 nm of 110 mW cm^{-2} white light through filters (KL45 + GG420), in 0.5 M KCl electrolyte solution containing dissolved O_2 and 1 mM MV^{2+}.
[c] Irradiation under −100 mV, in 0.5 M KCl electrolyte solution containing dissolved O_2 and 1 mM MV^{2+}, at 464 nm.
[d] Irradiation under −100 mV, pH = 2 dissolved O_2 and 5 mM MV^{2+}, at 464 nm.

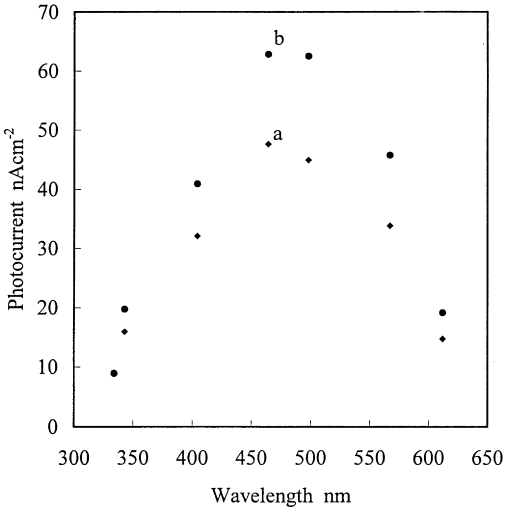

Fig. 3. Action spectrum of the QMV_3 monolayer film modified ITO electrode, photocurrent was measured at 464 nm under: (a) 0 mV and (b) −100 mV, respectively. The intensities of different wavelengths were all normalized.

measured under 0 and −100 mV bias voltage, respectively. The photocurrent maximum values were generated between 460 and 500 nm, which agreed with the maximum absorption of the QMV_3 LB film in 460–500 nm (Fig. 2), indicating that the aggregates of the dye in the LB film were responsible for photocurrent generation. To understand further the photocurrent generation process, some factors were investigated.

3.3. Bias voltage on the electrodes

The effect of bias voltage on photocurrent generation was investigated. Data show that when the bias voltage was applied on a QMV_3 monolayer modification ITO electrode, the photocurrent increases linearly with increasing negative potential, and vice versa. These phenomena were also observed for QMV and QMV_8. This is because the negative potential on the electrode can accelerate the separation of the electron–hole pairs and prolong the lifetime of the electron recombination in this system [11], leading to enhanced cathodic photocurrent. In the same time the dark current is meagre, indicating that the light sensitized dye molecules generate the current. When 1 mM MV^{2+} and O_2 are presented in the electrolyte solution, ca.100, 123 and 94 nA cm^{-2} photocurrent were obtained, under −100 mV bias voltage at 464 nm irradiation with a 1.14×10^{16} photos $cm^{-2}\,s^{-1}$ light intensity. In this case, the quantum yields reach ca. 0.68, 0.73 and 0.83% for QMV, QMV_3 and QMV_8, respectively (Table 1c). The open circuit photovoltage for the electrodes were measured also and they are 0.17, 0.23 and 0.19 V for QMV, QMV_3 and QMV_8, respectively.

3.4. Dependence on electron acceptors and donor concentration

When the electrodes were illuminated with 110 mW cm^{-2} white light and under −100, 0 and 100 mV bias voltage, respectively, in 0.5 M KCl electrolyte solution, the overall photocurrents increase with increasing concentration of MV^{2+}. At low concentrations of MV^{2+}, the photocurrents increase monotonically with the increasing of MV^{2+} concentration, and then reach saturation after 5 mM. At high concentrations, the electron transfer is mainly dependent on the concentration of the holes generated on the surface. Applying the negative bias voltage is favorable to the cathodic current generation, thus when bias voltage changes from 100 to −100 mV under the same conditions, the cathodic photocurrent was enhanced linearly, which is in agreement with the observance of the effect of bias voltage discussed above. These results clearly indicate that the photocurrent is limited by the migration of holes to the ITO electrode surface and the electron-transfer rate constant between the MV^{2+} and the photogenerated hole at the interface [12]. Experiments also found that dissolved oxygen, due to formation superoxide anion radical, is favorable to cathodic photocurrent [11]. The addition of an electron donor such as H_2Q will decrease the cathodic photocurrent and even change cathodic current into anodic photocurrent at high concentrations, suggesting that the existence of H_2Q is unfavorable to cathodic photocurrent generation.

3.5. Light intensity dependence of the photocurrent

Fig. 4 shows the intensity dependence of the photocurrent measured at the different potential vs. SCE for the QMV_3 LB film on ITO electrode, in 0.5 M KCl electrolyte solution containing 1 mM MV^{2+}. The equations are (a) $y = 33.1x^{0.81}$, (b) $y = 30.6x^{0.74}$ and (c) $y = 22.4x^{0.71}$ under −100, 0 and 100 mV, respectively. According to the suggestion of Donovan et al. [13], the photocurrent has a dependence on light intensity: $i = KI^m$, where $m = 1$ is characteristic of unimolecular recombination and $m = 1/2$ is the characteristic of bimolecular recombination. In our case, m values are 0.81, 0.74 and 0.71 under −100, 0 and 100 mV, respectively, indicating that the recombination of the separated charge in the dye LB film probably contains both of the above recombination (unimolecular and bimolecular) processes for the QMV_3 system. The difference in m values under different bias voltages suggests that the negative bias voltage is more favorable to unimolecular recombination process, while the positive bias voltage is more favorable to bimolecular recombination character. A similar dependence is also observed for QMV, and QMV_8, suggesting that they have the same relaxation modes as QMV_3.

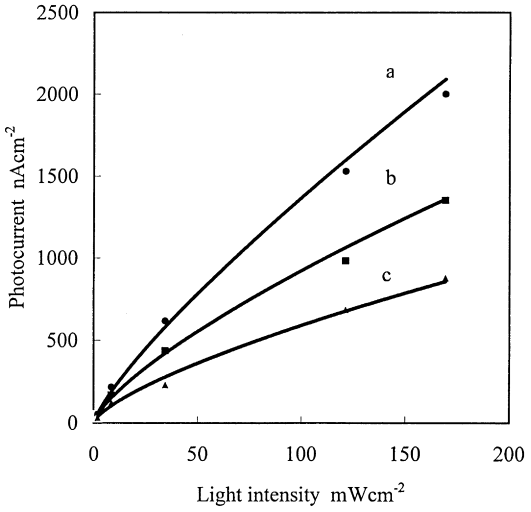

Fig. 4. Light intensity dependence of the photocurrent measured vs. SCE for the dye QMV_3 monolayer film on ITO electrode in 0.5 M KCl electrolyte solution containing 1 mM MV^{2+} under ambient condition: (a) −100 mV; (b) 0 mV; (c) 100 mV.

3.6. Dependence on pH Values

The effect of the pH value on photocurrent generation was investigated in a Britton–Robinson buffer solution containing 0.5 M KCl. Fig. 5 shows that the cathodic photocurrent generated from a QMV_3 modified ITO electrode was quickly increased when pH value was decreased, and vice versa under zero bias voltage (Fig. 5(b)). The data are fitted by an ideal titration curve [14]. Due to an equilibrium between –OH and $–O^-$ groups at the electrode surface,

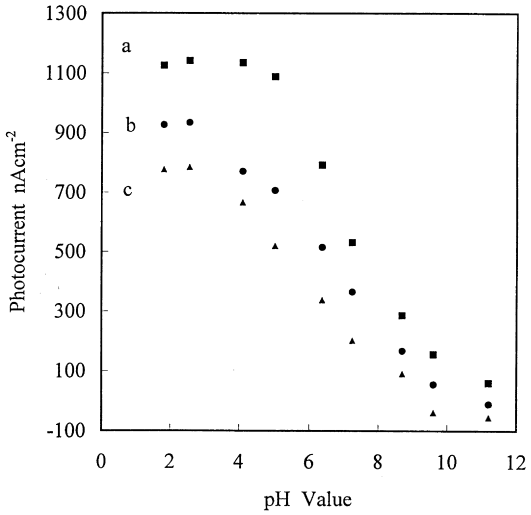

Fig. 5. The effect of pH on QMV_3-ITO electrode photocurrent in Britton–Kobison buffer solution containing 0.5 M KCl under ambient conditions, upon irradiation with a 110 mW cm^{-2} white light: (a) (■) −100 mV; (b) (●) 0 mV; (c) (▲) 100 mV.

[15] the acidic medium leads to an anodic shift of the flat-band potential of the ITO electrode, while the alkaline medium leads to the cathodic shift of the flat-band potential of the ITO electrode. The shifts in the flat-band potential will affect the injection of the electron from the ITO conduction band to the sensitized dye molecules, leading to changing photocurrent generation [16]. The relationship between the photocurrent and pH values were also determined under −100 and 100 mV as shown in Fig. 5(a) and (c), respectively, which is coincident with that for under-zero bias voltage. Comparing curve (b) with curves (a) and (c), it was known that the negative bias voltage is favorable to the cathodic current, which is coincident with the dependence of the photocurrent on the applied bias potential. Under favorable circumstances, pH ca. 2, in the presence of O_2 and 5 mM MV^{2+}, with −100mV bias voltage, then photocurrent ca. 105, 199 and 102 nA cm^{-2} were obtained under irradiation of 464 nm light with a 1.14×10^{16} photos $cm^{-2}\,s^{-1}$ light intensity, the quantum yields are 0.72, 1.19 and 0.90% for the QMV, QMV_3 and QMV_8, respectively (Table 1d).

3.7. Electrochemical properties of the dye

In order to estimate the LUMO of the dye molecules and discuss the mechanism of photocurrent generation, cyclic voltammetry experiments were cared out in a 0.5 M KCl aqueous solution, the monolayer dye-ITO was used as the working electrode. Oxygen was removed from the electrolyte solution by bubbling N_2 before every measurement. The experiment found that cyclic voltammetry of the dye monolayer films only had an oxidation potential peak, no reduction potential peak appeared, indicating that the redox reaction was irreversible on the ITO electrode.The oxidation peak potentials are 0.88, 0.99 and 0.93 V for QMV, QMV_3 and QMV_8, respectively.

3.8. Mechanism of photocurrent generation

In order to elucidate the mechanism of light sensitization for the cathodic and anodic photocurrent, the energies of the relevant electronic states must be estimated. Using the oxidation potential data obtained from the CV, together with the monolayer optical excitation, an energy level diagram can be constructed, as shown in Scheme 2 (schematic diagram showing the electron transfer processes: (a) cathodic photocurrent; (b) anodic photocurrent. QMV_3 and QMV_3^* stand for the ground state and excited state of the dye QMV_3, respectively; E_{fb} presents an anodic shift of the flat-band potential in the acidic medium).

From the electron affinity the conduction band (E_c) and valence band (E_v) edges of the ITO electrode surface are estimated to be ca. −4.5 and −8.3 eV, respectively [17]. The lowest levels available to accept an electron, and the first excited singlet state for the dye QMV_3 (as an example) film are assumed to be −5.73 (0.99 V vs. SCE) and

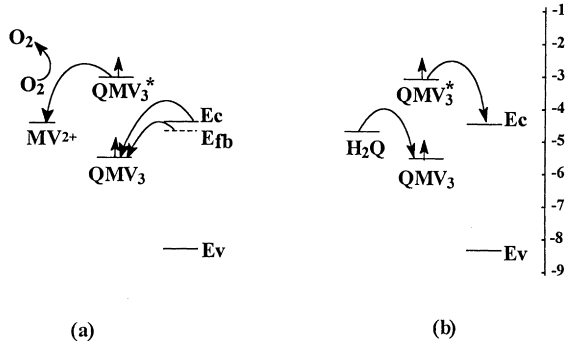

Scheme 2.

−3.19 eV on the absolute scale, respectively, with reference to oxidation potential of 0.99 V (vs. SCE) and band gap of 2.54 eV (488 nm). The reduction potential of MV^{2+} is −4.51 (−0.23 V vs. SCE), oxidation potential of H_2Q is −4.61 eV (−0.13 V vs. SCE), respectively, on the absolute scale [11].

It can be seen that the direction of the photocurrent depends not only on the dye sensitized by light, but also on the nature of the redox couples in the aqueous phase surrounding the electrode. If the electrolyte is favorable to accepting an electron, such as in the presence of O_2, MV^{2+} or an acidic medium, cathodic photocurrent is generated. If not, for example, a strong electron donor (H_2Q) can donate electrons to quench the excited aggregates, leading to anodic photocurrent generation [11].

4. Conclusions

1. Steady cathodic photocurrents were obtained from the dichromophore dye LB films fabricated ITO electrodes. A mechanism of photosensitive electron transfer was proposed which does not involve any essential change between the monochromophore and dichromophore dyes.
2. The limiting area of the QMV_3 only increases by 0.16 nm^2 when compared with QMV, implying that the magnitude of its active chromophores per area increases by 35%, taking into account that there are two chromophores in one molecule for QMV_3. The quantum yield of the QMV and the QMV_3 measured at 464 nm in 0.5 M KCl electrolyte solution containing dissolved O_2 and 1 mM $MV^{2+}$are 0.66 and 0.71%, respectively (Table 1b). The quantum yield of the QMV_3 only increases by 8%. Their quantum yields measured under favorable conditions (Table 1d) were 0.72 and 1.19%, respectively. The range of increase of the QMV_3 quantum yield is ca. 40%, indicating that the combination of two chromophores in one molecule such as QMV_3 has no obvious positive effect on the quantum yield, compared with the QMV.
3. The limiting area of the QMV_8 increases by a factor of two, consequently the magnitude of the active chromophores per area does not increase compared with QMV, but the quantum yield of the QMV_8 increases 25% under favorable conditions (Table 1d), compared with the QMV.
4. Comparing QMV with QMV_3 and QMV_8, due to having 4,4′-dipyrinum cation in the dichromophore molecules, the enhancement of the quantum yield is reasonable. Since the viologen derivative acts as a better electron acceptor in the system, it makes the charge separation more efficient in the dichromophore than in the mono-chromophore dyes. The molecular structure and the way of chromophore linkage play an important role in photocurrent generation.

Acknowledgements

The project is financially supported by the State Key Project for fundamental Research (G 1998061310) and National Nature Science Foundation of China (no. 29671001, 29601001, 59872001)

References

[1] G. Roberts, Sens. Actuators 4 (1984) 131.
[2] W. Arden, P. Fromherz, J. Electrochem. Soc. (1980) 127370.
[3] D. Noukakis, M. Van der Auweraer, F.C. De Schryver, J. Phys. Chem. 98 (1994) 11745.
[4] W.S. Xia, C.H. Huang, X.Z. Ye, C.P. Luo, L.B. Gan, Z.F. Liu, J. Phys. Chem. 100 (1996) 2244.
[5] A. Haran, D.H. Waldeck, R. Naaman, E. Moons, D. Cahen, Science 263 (1994) 948.
[6] G.J. Ashwell, G. Jefferies, C.D. George, R. Ranjan, R.B. Charters, R.P. Tatam, J. Mater. Chem. 6 (2) (1996) 131.
[7] G.J. Ashwell, P.D. Jackson, G. Jefferies, I.R. Gentle, C.H.L. Kennard, J. Mater. Chem. 6 (2) (1996) 137.
[8] A.D. Lang, J. Zhai, C.H. Huang, L.B. Gan, Y.L. Zhao, D.J. Zhou, Z.D. Chen, J. Phys. Chem. B102 (1998) 1424.
[9] D.G. Wu, C.H. Huang, L.B. Gan, Y.Y. Huang, Langmuir 14 (1998) 3783.
[10] W.F. Mooney, P.E. Brown, J.C. Russell, S.B. Costa, L.G. Pedersen, D.G. Whitten, J. Am. Chem. Soc. 106 (1984) 5659.
[11] Y.S. Kim, K. Liang, K.Y. Law, D.G. Whitten, J. Phys. Chem. 98 (1994) 984.
[12] Y. Gu, D.H. Waldeck, J. Phys. Chem. B 102 (1998) 9015.
[13] K.J. Donovan, R.V. Sudiwala, E.G. Wilson, Mol. Cryst. Liq. Cryst. 194 (1991) 337.
[14] P. Fromherz, W. Arden, J. Am. Chem. Soc. 102 (1980) 6211.
[15] S. Morrison, Electrochemistry at Semiconductors and Oxidized Metal Electrodes, Plenum Press, New York, 1980.
[16] G. Biesmans, M. Van der Auweraer, C. Cathry, D. Meerschaut, F.C. De Schryver, W. Storck, F. Willig, J. Phys. Chem. 95 (1991) 3771.
[17] L. Sereno, J.J. Silber, L. Otero, M.D.V. Bohorquez, A.L. Moore, T.A. Moore, D. Gust, J. Phys. Chem. 100 (1996) 814.